Multisource Least-squares Extended Reverse-time Migration with Preconditioning Guided Gradient Method

Yujin Liu[*†]*, William W. Symes*[†] *and Zhenchun Li*[*]*, *[*]*China University of Petroleum (Huadong),*[†]*Rice University*

SUMMARY

Least-squares reverse-time migration (LSRTM) provides image of reflectivity with high resolution and compensated amplitude, but the computational cost is extremely high. One way to improve efficiency is to encode all of shot gathers into one or several super-shot gathers with designed encoding functions so as to solve a smaller number of wave-equations at each iteration. Another way is to use different kinds of preconditioners to accelerate the convergent rate of iterations. In this abstract, we combine these two methods together and extend them into prestack imaging, which we call extended reverse-time migration (ERTM). The sparsity of reflectivity is used as prior information and preconditioning guided gradient (PGG) method is developed to suppress crosstalk introduced by phase encoding and improve resolution of the extended image in the subsurface offset domain. Numerical tests on SEG/EAGE salt model show that our proposed method can provide a more reliable extended image with almost the same cost of ERTM, which makes the method valuable in migration velocity analysis and AVO/AVA analysis.

INTRODUCTION

The general procedure of wave-equation migrations can be divided into two steps, the first one is wavefield reconstruction, i.e., forward-propagate source wavefield and back-propagate receiver wavefield, the second one is to apply imaging condition to these two wavefields at each depth to get the image of subsurface image (Claerbout, 1971). Compared with propagators derived from ray theory or one-way wave equation, the propagator of reverse-time migration is derived directly from two-way wave equation, so it's the most accurate one. However, as cross-correlation imaging condition is only the adjoint of forward modeling operator (Lailly, 1983), it will generate low-frequency noise, imbalanced amplitude and decreased resolution.

One way to solve above problems is to cast reflectivity imaging as a least-squares inverse problem and solve it iteratively using gradient category methods, which is often called least-squares migration (LSM) (Tarantola, 1984; Nemeth et al., 1999; Kühl and Sacchi, 2003; Clapp, 2005; Valenciano et al., 2006). As two times of full RTM approximately needs to perform at each iteration of LSM, the computational cost of LSM is extremely high. There are several ways to decrease computational cost. One way is to compress seismic data using phase encoding method (Morton and Ober, 1998; Romero et al., 2000; Zhang et al., 2005; Liu et al., 2006; Tang, 2009; Godwin and Sava, 2010; Gao et al., 2010; Schuster et al., 2011; Herrmann and Li, 2011), such as random phase encoding, plane-wave phase encoding, amplitude encoding, deterministic source encoding. Another way is using preconditioner to accelerate the convergent rate of iteration, such as approximated diagonal of Hessian (Pratt, 1999; Shin et al., 2001; Tang and Lee, 2010), deblurring filter (Aoki and Schuster, 2009), image-guided filter(Ma et al., 2010) and so on.

In this abstract, We implement multisource LSERTM and use an approximation of diagonal Hessian in the subsurface offset domain as a preconditioner to reduce the inversion cost. A modified gradient method, namely preconditioned conjugate guided gradient (PGG), is also developed to test the effect of crosstalk introduced by phase encoding on different norms of model residual. Numerical tests on SEG/EAGE demonstrate that a more robust inversion result of extended reflectivity can be obtained efficiently by our proposed method.

THEORY

In this section, we will give the formulas of extended linearized Born modeling (ELBM), extended reverse-time migration (ERTM), approximation of diagonal of Hessian, least-squares extended reverse-time migration (LSERTM) and implementation of preconditioning guided gradient (PGG) algorithm.

Extended reverse-time migration with phase encoding

In acoustic constant density medium, seismic wave propagation can be expressed in frequency domain as follows:

$$(\nabla^2 + \omega^2 m(\mathbf{x},z))u(\mathbf{x},z,\omega) = f(\omega)\delta(\mathbf{x}-\mathbf{x}_s) \tag{1}$$

where $\mathbf{x}$ is the horizontal vector, z is the depth axis, $\mathbf{x}_s$ is the source position, $m(\mathbf{x},z)$ is squared slowness, $u(\mathbf{x},z,\omega)$ is the seismic wavefiled at freqency ω, $f(\omega)$ is the spectrum of source function. We should note that $m(\mathbf{x},z)$ is a scaler here.

Based on the idea of model extension and extended modeling (Symes, 2008), equation 1 changes to:

$$\nabla^2 u(\mathbf{x},z,\omega) + \omega^2 \int \mathrm{d}\mathbf{y} m(\mathbf{x},\mathbf{y},z)u(\mathbf{y},z,\omega) = f(\omega)\delta(\mathbf{x}-\mathbf{x}_s) \tag{2}$$

where $m(\mathbf{x},\mathbf{y},z)$ becames an operator. When $m(\mathbf{x},z) = m(\mathbf{x},\mathbf{y},z)\delta(\mathbf{x}-\mathbf{y})$, equation 2 is degraded into equation 1.

Split the extended model into two parts as follows:

$$m(\mathbf{x},\mathbf{y},z) = b(\mathbf{x},z)\delta(\mathbf{x}-\mathbf{y}) + r(\mathbf{x},\mathbf{y},z) \tag{3}$$

where $b(\mathbf{x},z)$ is background velocity and $r(\mathbf{x},\mathbf{y},z)$ is extended reflectivity. Correspondingly, $u(\mathbf{x},\mathbf{y},z,\omega) = u_0(\mathbf{x},\mathbf{y},z,\omega) + \delta u(\mathbf{x},\mathbf{y},z,\omega)$, then after linearized approximation, equation 2 changes to the following two equations:

$$(\nabla^2 + \omega^2 b(\mathbf{x},z))u_0(\mathbf{x},z,\omega) = f(\omega)\delta(\mathbf{x}-\mathbf{x}_s) \tag{4}$$

$$(\nabla^2 + \omega^2 b(\mathbf{x},z))\delta u(\mathbf{x},z,\omega) = -\omega^2 \int \mathrm{d}\mathbf{y} r(\mathbf{x},\mathbf{y},z)u_0(\mathbf{y},z,\omega) \tag{5}$$

The solution of equation 4 can be written as:

$$u_0(\mathbf{x},z,\omega) = f(\omega)G(\mathbf{x},\mathbf{x}_s,\omega) \tag{6}$$

Where $G(\mathbf{x},\mathbf{x}_s,\omega)$ is the Green function with the source at $\mathbf{x}_s$. Seismic data $d(\mathbf{x}_r,\mathbf{x}_s,\omega)$ can be approximated modeled by the solution $\delta u(\mathbf{x},z,\omega)$ of equation 5 at the predefined source locations $\mathbf{x}_s$ and receiver locations $\mathbf{x}_r$. Define $\mathbf{y} = \mathbf{x}+\mathbf{2h}$, replace $\mathbf{x}$ with $\mathbf{x}-\mathbf{h}$ and assuming $z_s = z_r = 0$, The modeling formula can be expressed as:

$$d(\mathbf{x}_r,\mathbf{x}_s,\omega) = \\ -\omega^2 f(\omega)\int \mathrm{d}\mathbf{x}\mathrm{d}\mathbf{h}\, G(\mathbf{x}_r,\mathbf{x}+\mathbf{h},\omega)r(\mathbf{x},\mathbf{h})G(\mathbf{x}-\mathbf{h},\mathbf{x}_s,\omega) \tag{7}$$

which we call extended linearized Born modeling (ELBM) fomula. Correspondingly, we can write the adjoint of ELBM as follows:

$$r(\mathbf{x},\mathbf{h}) = \\ -\int \mathrm{d}\mathbf{x_s}\mathrm{d}\mathbf{x_r}\mathrm{d}\omega\,\omega^2 f^*(\omega)G^*(\mathbf{x}_s,\mathbf{x}-\mathbf{h},\omega)G^*(\mathbf{x}+\mathbf{h},\mathbf{x}_r,\omega)d(\mathbf{x}_r,\mathbf{x}_s,\omega) \tag{8}$$

We can see that equation 8 is actually the space shift imaging condition (Rickett and Sava, 2002; Biondi and Symes, 2004). For the fake of simplicity, we call it extended reverse time migration (ERTM) formula in the following derivations.

From the equation 8, we can also see that the computational cost of ERTM is very high and is proportional to the number of sources. In order to decrease the computation cost of migration, multisource migration was proposed to compress the seismic data. There are several kind of schemes commonly used in seismology, such as random phase encoding (Romero et al., 2000), plane-wave phase encoding (Liu et al., 2006) and amplitude encoding (Godwin and Sava, 2010). It has been shown that the single-sample random time phase shift encoding function seems to give the best convergent result (Krebs et al., 2009), so we adapt this scheme in our abstract. The encoding function is defined as follows:

$$\alpha(\mathbf{x_s},p_s) = \frac{1}{\sqrt{N}}\gamma(\mathbf{x_s},p_s) \tag{9}$$

where p_s is the realization index, N is the number of realization and γ is a random sequence of signs, i.e. $+1$ and -1. Seismic data after encoding is:

$$\tilde{d}_{obs}(\mathbf{x}_r,p_s,\omega) = \int \mathrm{d}\mathbf{x_s}\,\alpha(\mathbf{x}_s,p_s)d_{obs}(\mathbf{x}_r,\mathbf{x}_s,\omega) \tag{10}$$

Correspondingly, the same encoding function is used to encode the sources. As the wave-propagator is linear with the input source, so the source wavefield can be calculated from original formula but with the encoded source, that is:

$$S(\mathbf{x},p_s,\omega) = \int \mathrm{d}\mathbf{x_s}\alpha(\mathbf{x}_s,p_s)f(\omega)G(\mathbf{x},\mathbf{x}_s,\omega) \tag{11}$$

As the wave-propagator is linear with the input source, so we just need to change the source in order to simulate seismic data corresponding the encoded one. The formula of ELBM with encoded source is:

$$\tilde{d}(\mathbf{x}_r,p_s,\omega) = \\ -\omega^2\int \mathrm{d}\mathbf{x}\mathrm{d}\mathbf{h}G(\mathbf{x}_r,\mathbf{x}+\mathbf{h},\omega)r(\mathbf{x},\mathbf{h})S(\mathbf{x}-\mathbf{h},p_s,\omega) \tag{12}$$

The formula of ERTM with phase encoding can be written as follows:

$$r(\mathbf{x},\mathbf{h}) = \\ -\int \mathrm{d}p_s\mathrm{d}\mathbf{x_r}\mathrm{d}\omega\,\omega^2 S^*(p_s,\mathbf{x}-\mathbf{h},\omega)G^*(\mathbf{x}+\mathbf{h},\mathbf{x}_r,\omega)\tilde{d}(\mathbf{x}_r,p_s,\omega) \tag{13}$$

The number of encoding realization N is often much smaller than the number of sources, so the computational cost of ERTM is greatly reduced.

Preconditioner: approximation of diagonal of Hessian

Diagonal of Hessian in the subsurface offset domain can be written as (Valenciano et al., 2006):

$$D(\mathbf{x},\mathbf{h}) = \int \mathrm{d}\mathbf{x}_s\mathrm{d}\mathbf{x}_r\mathrm{d}\omega\,\omega^4|f(\omega)|^2\,|G(\mathbf{x}-\mathbf{h},\mathbf{x}_s,\omega)|^2|G(\mathbf{x}+\mathbf{h},\mathbf{x}_r,\omega)|^2. \tag{14}$$

Similarly, we can encode receiver wavefield after define phase encoding function $\beta(\mathbf{x_r},p_r) = \frac{1}{N}\gamma(\mathbf{x_r},p_r)$,

$$R(\mathbf{x},p_r,\omega) = \int \mathrm{d}\mathbf{x}_r\,\beta(\mathbf{x}_r,p_r)G(\mathbf{x},\mathbf{x}_r,\omega). \tag{15}$$

then we can approximate equation 14 as,

$$\widetilde{D}(\mathbf{x},\mathbf{h},p_r) = \int \mathrm{d}\mathbf{x}_s\mathrm{d}\omega\omega^4|f(\omega)|^2|G(\mathbf{x}-\mathbf{h},\mathbf{x}_s,\omega)R(\mathbf{x}+\mathbf{h},p_r,\omega)|^2. \tag{16}$$

With the encoded source wavefield defined in equation 11, equation 16 can be simplified as:

$$\widetilde{\widetilde{D}}(\mathbf{x},\mathbf{h},p_s,p_r) = \int \mathrm{d}\omega\,\omega^4|S(\mathbf{x}-\mathbf{h},p_s,\omega)R(\mathbf{x}+\mathbf{h},p_r,\omega)|^2. \tag{17}$$

Commonly, the receiver-side term is often discarded in order to decrease the computational cost, the result is often called source wavefield intensity (SWI). The justification of SWI is based on the assumption that receivers spread all over the model, which is not the fact. Another more accurate approximation is replacing the receiver-side term with source-side term based on the assumption that all the position of receivers was replaced by sources, that is:

$$\widetilde{D}_{SS}(\mathbf{x},\mathbf{h},p_s) = \int \omega\,\omega^4|S(\mathbf{x}-\mathbf{h},p_s,\omega)|^2|S(\mathbf{x}+\mathbf{h},p_s,\omega)|^2. \tag{18}$$

It has shown that this approximation is more accurate than SWI and seems to be accurate enough as a preconditioner in least-squares inversion (Tang and Lee, 2010). Here we extend it to subsurface offset domain in order to accelerate the convergent rate of least-squares extended reverse-time migration (LSERTM).

Multisource least-squares extended reverse-time migration

Equation 12 can be written in a compact form as:

$$\tilde{\mathbf{d}} = \tilde{\mathbf{L}}\mathbf{m} \tag{19}$$

with regularization term, the objective function of LSM can be written as:

$$min_{\mathbf{m}} J_{LSM}[\mathbf{m}] = \frac{1}{2} \parallel \tilde{\mathbf{L}}\mathbf{m} - \tilde{\mathbf{d}}_{obs} \parallel_p + \frac{\sigma}{2} \parallel \mathbf{A}\mathbf{m} \parallel_p \tag{20}$$

where $\| \cdot \|_p$ denotes ℓ^p norm with $1 \leq p \leq 2$, $\mathbf{A}$ is regularization operator. The least-squares solution is only a member of a family of generalized ℓ^p-norm solutions that are deduced from a maximum-likelihood formulation. Among the various ℓ^p-norm solutions, the ℓ^1-norm solution is more robust than the ℓ^2-norm solution, because it is less sensitive to spiky, high-amplitude noise (Gersztenkorn et al., 1985; Scales et al., 1988; Claerbout and Muir, 1973; Taylor et al., 1979). In order to take advantages of both ℓ^2 and ℓ^1 norm solutions, hybrid ℓ^1/ℓ^2 - norm solutions are also tried (Huber, 1973; Bube and Langan, 1997; Guitton and Symes, 2003).

Iteratively reweighted least-squares (IRLS) method is a good choice to solve equation 20, but it require to compute weighting function at the outer loop of conjugate gradient iterations, which makes it expensive. Another variant of IRLS method, namely CGG method, guides the gradient to the imposed direction, is more efficient than IRLS(Ji, 2006).

In our implementation, we adapt the approximation of diagonal Hessian in the last section as preconditioner in the loop of CGG method, which we call preconditioning guided gradient (PGG) method. The complete algorithm of mutisource least-squares extended revere-time migration with PGG method is shown in 1 as follows:

Algorithm 1 MLSERTM with PGG

1: **for** $k = 0 \cdots niter$ **do**
2: generate random squence of signs γ
3: encode sources and data to get $\tilde{\mathbf{L}}$ and $\tilde{\mathbf{d}}_{obs}$
4: $\mathbf{r}^k = \tilde{\mathbf{L}}\hat{\mathbf{m}}^k - \tilde{\mathbf{d}}_{obs}$
5: compute $\hat{\mathbf{W}}_r^k$
6: compute $\hat{\mathbf{W}}_m^k$
7: $\mathbf{dm}^k = \hat{\mathbf{W}}_m^{T,k} \tilde{\mathbf{D}_{SS}}^{-1} \tilde{\mathbf{L}}^T \hat{\mathbf{W}}_r^{T,k} \mathbf{r}^k$
8: $\mathbf{dr}^k = \tilde{\mathbf{L}}\mathbf{dm}^k$
9: $\alpha_k = \frac{\langle \mathbf{dr}^k, \mathbf{r}^k \rangle}{\langle \mathbf{dr}^k, \mathbf{dr}^k \rangle}$
10: $\mathbf{m}^{k+1} = \mathbf{m}^{k+1} - \alpha_k \mathbf{dm}^k$
11: **end for**

NUMERICAL TEST

In this part, SEG/EAGE salt model is used for our numerical tests. The spatial sampling for both spatial axses is 30 m. Figure 1(a) shows the salt velocity model. The reflectivity model, calculated from velocity model using equation 3, is shown in Figure 1(b). A Ricker wavelet with a fundamental frequency of 15 Hz and temporal sampling of 1 ms is used to model the seismic data. 163 sources are evenly deployed on the surface with the sampling interval of 120 m and all of sources share the same 645 receivers with the sampling interval of 30 m on the surface. The synthetic data is generated by Born modeling operator with a time-domain finite-difference method.

Figure 2(a) shows the result of RTM, we can see that it is dominated by low-freqency noise. After applying laplacian filter, low-frequency noise was eliminated but the amplitude of the result is still imbalanced and very different from the true reflectivity model, as shown in figure 2(b). Next, We ran Multi-source LSRTM without any precondtioning for 163 iterations, which equals to the total number of sources, the result is shown in figure 2(c). By comparing figure 2(b) and 2(c), we can see that MLSRTM gives much better results. Figure 2(d) shows the approximated diagonal of Hessian with equation 18, we can see that the illumination under the salt is uneven caused by the complex salt body and limited acquisition geometry. Using figure 2(d) as a preconditioner, we can accelerate the convergent rate of LSRTM, the accelerated inversion result is shown in figure 2(e). Compared with figure 2(c) and 2(e), we can see that the amplitude of accelerated inversion result is more balanced, especially under the salt. Moreover, MLSRTM with different norm on model residual is also tested, Figure 2(f) shows the result using $\ell_{1.5}$ on model residual. From the result, we can see the S/N is higher than the result of ℓ_2 norm as shown in figure 2(e).

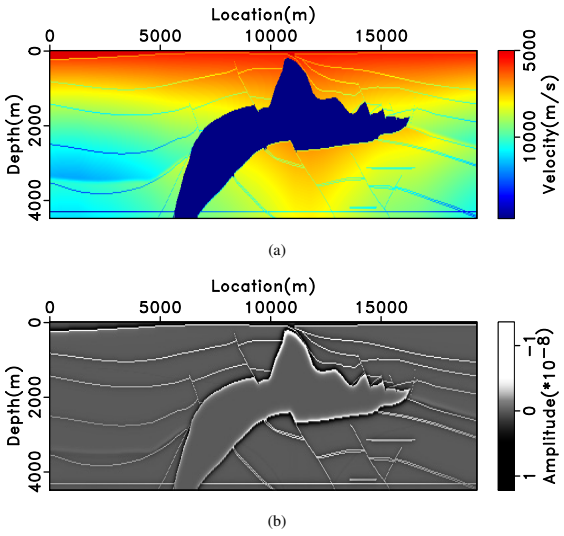

Figure 1: (a) velocity model; (b) reflectivity.

Next, we ran MLSERTM to see the effect of crosstalk introduced by phase encoding on prestack imaging. Figure 3(a) shows the approximated diagonal of Hessian in the subsurface offset domain, we can also see the uneven illumination under the salt and some energy smear around non-zero offset. Figure 3(b) shows the result of MLSERTM with ℓ_2 norm. Comparing figure 2(e) and figure 3(b), we can see that, the extended image is more prone to crosstalk introduced by phase encoding. That's reasonable because the extended model allows another degree of flexibility on the solution. After using PGG method to solve the ℓ_1 problem, we get the result as shown in figure 3(c). The result is much better than the result using ℓ_2 norm.

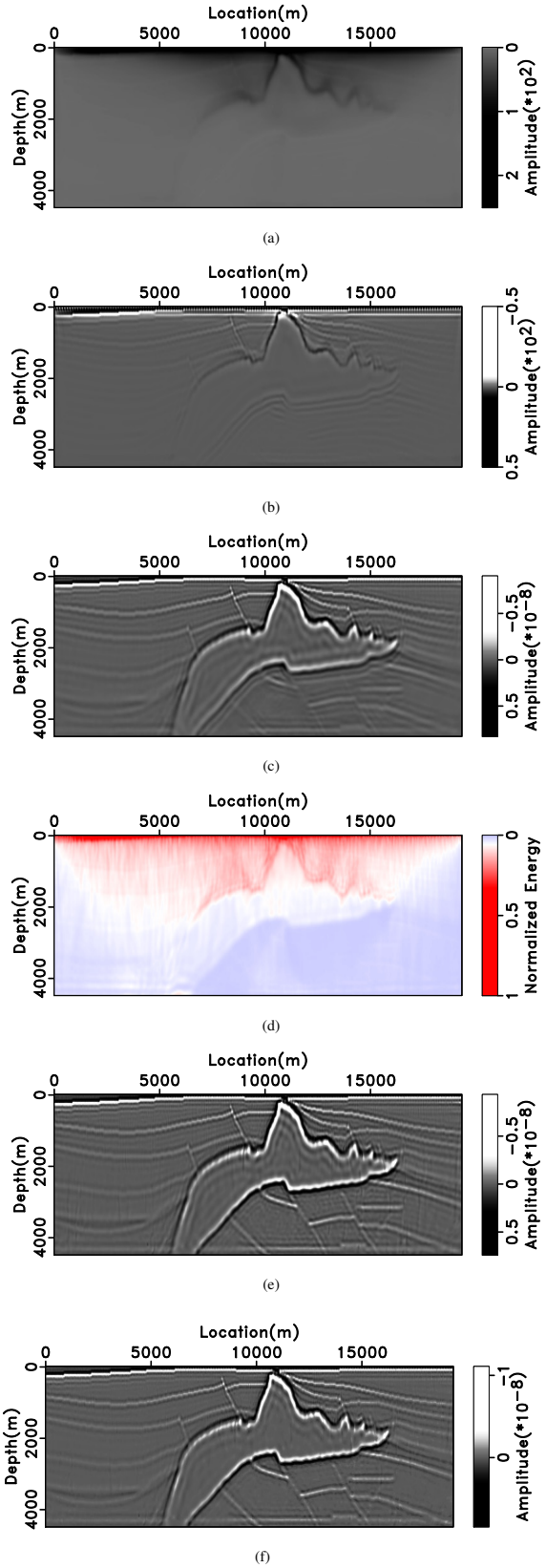

Figure 2: (a) RTM; (b) RTM after Laplacian filtering; (c) LSRTM without preconditioning; (d) Approximated diagonal Hessian; (e) LSRTM with conditioning; (f) LSRTM with preconditioning and sparsity-promotion.

CONCLUSION AND DISCUSSION

In this abstract, we develop LSERTM with PGG method, which can be used to solve ℓ_p norm problem flexibly and efficiently. With phase encoding method and approximated diagonal of Hessian as preconditioner, we can get the inversion result of extended reflectivity in the subsurface offset domain at the cost of ERTM but with more balanced amplitude and higher resolution, which is useful in the following migration velocity analysis and AVO/AVA analysis.

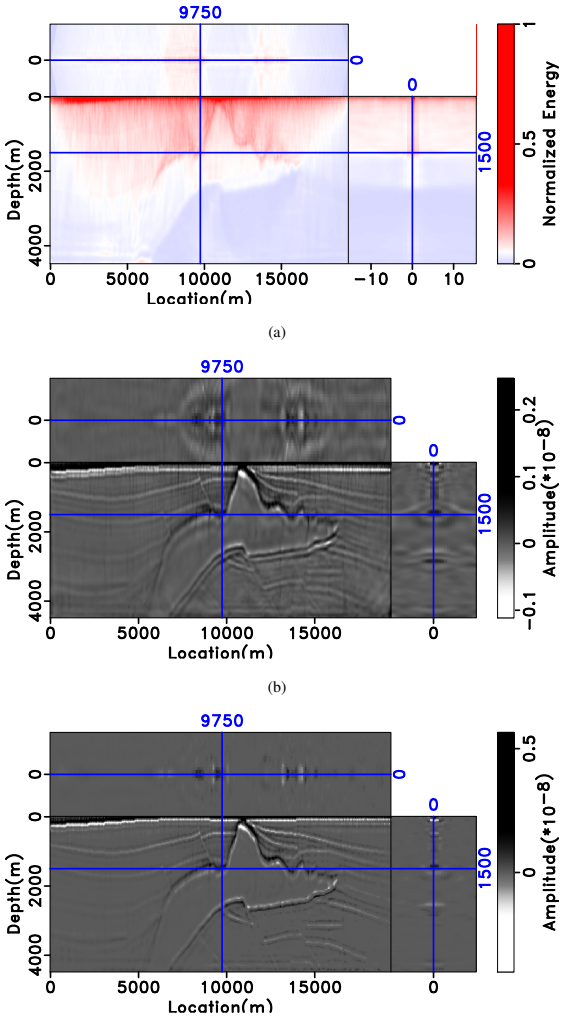

Figure 3: (a) Approximated diagonal Hessian in subsurface offset domain; (b) LSERTM with preconditioning; (c) LSERTM with preconditioning and sparsity-promotion.

ACKNOWLEDGMENTS

The work of first author is supported by China Scholarship Council during his visit to Rice University. YL thank The Rice Inversion Project (TRIP) for hosting him. YL and WWS thank the sponsors of TRIP for their support.

REFERENCES

Aoki, N., and G. T. Schuster, 2009, Fast least-squares migration with a deblurring filter: Geophysics, **74**, WCA83–WCA93.

Biondi, B., and W. W. Symes, 2004, Angle-domain common-image gathers for migration velocity analysis by wavefield-continuation imaging: Geophysics, **69**, 1283–1298.

Bube, K. P., and R. T. Langan, 1997, Hybrid l 1/l 2 minimization with applications to tomography: Geophysics, **62**, 1183–1195.

Claerbout, J. F., 1971, Toward a unified theory of reflector mapping: Geophysics, **36**, 467–481.

Claerbout, J. F., and F. Muir, 1973, Robust modeling with erratic data: Geophysics, **38**, 826–844.

Clapp, M. L., 2005, Imaging under salt: illumination compensation by regularized inversion: PhD thesis, Citeseer.

Gao, F., A. Atle, and P. Williamson, 2010, Full waveform inversion using deterministic source encoding: Presented at the 2010 SEG Annual Meeting.

Gersztenkorn, A., J. B. Bednar, and L. R. Lines, 1985, Robust iterative inversion for the one-dimensional acoustic wave equation: Presented at the 1985 SEG Annual Meeting.

Godwin, J., and P. Sava, 2010, Simultaneous source imaging by amplitude encoding: Technical report, Citeseer.

Guitton, A., and W. W. Symes, 2003, Robust inversion of seismic data using the huber norm: Geophysics, **68**, 1310–1319.

Herrmann, F. J., and X. Li, 2011, Efficient least-squares migration with sparsity promotion: EAGE, EAGE Technical Program Expanded Abstracts.

Huber, P. J., 1973, Robust regression: asymptotics, conjectures and monte carlo: The Annals of Statistics, **1**, 799–821.

Ji, J., 2006, Cgg method for robust inversion and its application to velocity-stack inversion: Geophysics, **71**, R59–R67.

Krebs, J. R., J. E. Anderson, D. Hinkley, R. Neelamani, S. Lee, A. Baumstein, and M.-D. Lacasse, 2009, Fast full-wavefield seismic inversion using encoded sources: Geophysics, **74**, WCC177–WCC188.

Kühl, H., and M. D. Sacchi, 2003, Least-squares wave-equation migration for avp/ava inversion: Geophysics, **68**, 262–273.

Lailly, P., 1983, The seismic inverse problem as a sequence of before stack migrations: Conference on inverse scattering: Theory and application, Society for Industrial and Applied Mathematics, Philadelphia, PA, 206–220.

Liu, F., D. W. Hanson, N. D. Whitmore, R. S. Day, and R. H. Stolt, 2006, Toward a unified analysis for source plane-wave migration: Geophysics, **71**, S129–S139.

Ma, Y., D. Hale, Z. Meng, and B. Gong, 2010, Full waveform inversion with image-guided gradient: Presented at the 2010 SEG Annual Meeting.

Morton, S. A., and C. C. Ober, 1998, Fastershot-record depth migrations using phase encoding: Presented at the 1998 SEG Annual Meeting.

Nemeth, T., C. Wu, and G. T. Schuster, 1999, Least-squares migration of incomplete reflection data: Geophysics, **64**, 208–221.

Pratt, R. G., 1999, Seismic waveform inversion in the frequency domain i theory and verification in a physical scale model: Geophysics, **64**, 888–901.

Rickett, J. E., and P. C. Sava, 2002, Offset and angle-domain common image-point gathers for shot-profile migration: Geophysics, **67**, 883–889.

Romero, L. A., D. C. Ghiglia, C. C. Ober, and S. A. Morton, 2000, Phase encoding of shot records in prestack migration: Geophysics, **65**, 426–436.

Scales, J. A., A. A. Gersztenkorn, S. A. Treitel, and L. R. Lines, 1988, Robust optimization methods in geophysical inverse theory: Presented at the 1988 SEG Annual Meeting.

Schuster, G., X. Wang, Y. Huang, W. Dai, and C. Boonyasiriwat, 2011, Theory of multisource crosstalk reduction by phase-encoded statics: Geophysical Journal International, **184**, 1289–1303.

Shin, C., S. Jang, and D.-J. Min, 2001, Improved amplitude preservation for prestack depth migration by inverse scattering theory: Geophysical prospecting, **49**, 592–606.

Symes, W. W., 2008, Migration velocity analysis and waveform inversion: Geophysical Prospecting, **56**, 765–790.

Tang, Y., 2009, Target-oriented wave-equation least-squares migration/inversion with phase-encoded hessian: Geophysics, **74**, WCA95–WCA107.

Tang, Y., and S. Lee, 2010, Preconditioning full waveform inversion with phase-encoded hessian: Presented at the 2010 SEG Annual Meeting.

Tarantola, A., 1984, Inversion of seismic reflection data in the acoustic approximation: Geophysics, **49**, 1259–1266.

Taylor, H. L., S. C. Banks, and J. F. McCoy, 1979, Deconvolution with the l 1 norm: Geophysics, **44**, 39–52.

Valenciano, A. A., B. Biondi, and A. Guitton, 2006, Target-oriented wave-equation inversion: Geophysics, **71**, A35–A38.

Zhang, Y., J. Sun, C. Notfors, S. H. Gray, L. Chernis, and J. Young, 2005, Delayed-shot 3d depth migration: Geophysics, **70**, E21–E28.